



Published in final edited form as:

J Nutr Biochem. 2015 December ; 26(12): 1589–1598. doi:10.1016/j.jnutbio.2015.07.026.

Amino Acid Starvation Induced by Protease Inhibition Produces Differential Alterations in Redox Status and the Thiol Proteome in Organogenesis-Stage Rat Embryos and Visceral Yolk Sacs

Craig Harris¹, Joseph L. Jilek¹, Karilyn E. Sant¹, Jan Pohl³, Matthew Reed³, and Jason M. Hansen²

¹Toxicology Program, Department of Environmental Health Sciences, University of Michigan, Ann Arbor, Michigan 48109-2029

²Department of Physiology and Developmental Biology, Brigham Young University, Provo Utah, 84602

³Biotechnology Core Facility Branch, Centers for Disease Control/DSR Atlanta, Georgia 30333

Abstract

The process of embryonic nutrition in rodent conceptuses during organogenesis has been shown to involve a dominant histiotrophic mechanism where essential developmental substrates and micronutrients are supplied as whole maternal proteins or cargoes associated with proteins. The histiotrophic nutrition pathways (HNP) responsible for uptake and initial processing of proteins across maternal-conceptal interfaces involve uptake via receptor mediated endocytosis and protein degradation via lysosomal proteolysis. Chemical inhibition of either process can lead to growth deficits and malformation in the embryo (EMB), but selective inhibition of either HNP component will elicit a different subset of developmental perturbations. In vitro, whole embryo culture (WEC) exposure of GD10 or GD11 rat conceptuses to the natural protease inhibitor, leupeptin, leads to significant reductions in all measured embryonic growth parameters as well as a myriad of other effects. Leupeptin doses of 10 μ M or 20 μ M over a 26 hr period (GD10-GD11) and 50 μ M over a 3 hr pulse period produced significant decreases in the clearance of FITC-albumin from culture media. The near complete loss of acid soluble fluorescence and increased total visceral yolk sac (VYS) protein content confirmed the selective inhibition of proteolysis. Inhibition of lysosomal proteolysis thus deprives the developing EMB of essential nutrient amino acids producing conditions akin to amino acid starvation, but may also cause direct effects on pathways critical for normal growth and differentiation. Following leupeptin exposure for 26 or 6 hr, total glutathione (GSH) concentrations dropped significantly in the VYS, but only slightly in yolk sac (YSF) and amniotic (AF) fluids. Cys concentrations increased in VYS and EMB, but dropped in YSF and AF fluids. Redox potentials (E_h) for the GSSG/GSH redox couple trended significantly toward the

Corresponding Author: Dr. Craig Harris, Toxicology Program, Department of Environmental Health Sciences, University of Michigan, 1420 Washington Heights, Ann Arbor, Michigan 48109-2029, (Tel) 734 936-3397, (Fax) 734 763-8095, charris@umich.edu.

Publisher's Disclaimer: This is a PDF file of an unedited manuscript that has been accepted for publication. As a service to our customers we are providing this early version of the manuscript. The manuscript will undergo copyediting, typesetting, and review of the resulting proof before it is published in its final citable form. Please note that during the production process errors may be discovered which could affect the content, and all legal disclaimers that apply to the journal pertain.

positive, confirming the net oxidation of conceptual tissues following leupeptin treatment. Analysis of the thiol proteome showed few alterations to specific pathways mapped to the KEGG Pathway database, but did reveal significant increases in concentrations of proteins associated with glycolysis/gluconeogenesis in the VYS and decreased concentrations proteins associated with ribosome biogenesis and function in the EMB. A subset of proteins elevated by >2-23 fold in the VYS were identified as serum (blood) proteins and represent the maternal-side proteins captured by the VYS and which are not degraded in the lysosomes as a result of leupeptin's inhibitory action. The observed constellation of proteins decreased in the EMB by leupeptin represent proteins from several adaptive pathways that are commonly altered in responses to amino acid starvation. These studies show clear differential responses to protease inhibition in VYS and EMB during organogenesis and suggest the possibility for additional roles of redox regulation, cellular adaptations and metabolic insufficiency caused by protease inhibition.

Keywords

embryo; visceral yolk sac; histiotrophic nutrition; leupeptin; glutathione; cysteine; redox potential; isotope coded affinity tags (ICAT); thiol proteome; amino acid starvation

INTRODUCTION

Embryonic nutrition during the growth and differentiation-sensitive phase of rodent organogenesis has been shown to be exclusively dependent on the capture and uptake of nutrients through histiotrophic nutrition pathways (HNP) by the visceral yolk sac (VYS) endoderm [1-6]. All mammalian conceptuses possess a functional VYS during this critical phase of development where programmed rapid growth and differentiation guide the structural and functional biogenesis of all systems required for a normal embryo and fetus. Studies in rodents, which have a non-vestigial inverted VYS that completely encompasses the developing embryo throughout gestation, have shown that the HNP functions of receptor-mediated endocytosis (RME), primary vesicular formation, and lysosomal proteolysis are necessary to capture bulk protein from the immediate surrounding maternal fluids for degradation in the lysosomes in order to supply the growing embryo with required amino acids, as well as to supply other lipids, cofactors, and growth factors, bound to their appropriate proteins carriers as cargoes [7-11]. Exclusive reliance on the HNP axis for nutrient supply and processing raises the possibility that the transporters, structural proteins, regulators and enzymes of this pathway could be potential targets for mediating embryotoxicity and the elicitation of structural and functional birth defects.

Previous studies have characterized the effects of known dysmorphogens and chemical inhibitors of RME and lysosomal proteolysis in the characterization of HNP in rodents [12-15]. Although embryotoxic agents such as ethanol have been shown to have a selective inhibitory effect on RME, the majority of studies have focused on the inhibition of lysosomal proteolysis by several different types of chemicals [16]. Lysosomal inhibitors such as chloroquine [14], selective cathepsin inhibitors, such as Z-Phe-Ala-CHN₂ [12], and broad-spectrum cysteine, serine and threonine inhibitors, such as leupeptin [10, 17, 18], have all been shown to disrupt HNP activity and alter normal embryonic growth and

development. Gross developmental consequences of protease inhibition have been well documented at the biochemical level, but very little is known about the specific mechanisms and molecular pathways that are impacted by the induced amino acid starvation.

Leupeptin (N-acetyl-L-leucyl-L-leucyl-L-arginal) is a naturally occurring microbial protease produced by the Gram-positive bacteria (*Streptomyces*; actinomycetes), which are naturally found in the soil [19, 20]. The endopeptidase, leupeptin, differs from most other natural protease inhibitors because it contains an acetyl group and possesses an arginal aldehyde in place of the more common terminal carbonyl. Unlike most of its synthetic protease counterparts, leupeptin is believed to be much less toxic to humans and has generated considerable interest as a possible therapeutic intervention for purposes as diverse as the treatment of hearing loss (10 μ M -100 μ M)[21, 22], treatment of malaria [23], HIV [24, 25], or anywhere protease inhibition may be otherwise indicated[26]. Direct exposure of organogenesis-stage rat and mouse conceptuses grown in whole embryo culture (rWEC) to leupeptin (10 μ M -100 μ M) resulted in a significant accumulation of undigested protein in the lysosomes (~80% increase) and the significant reduction of growth and widespread dysmorphogenesis [17]. The initial characterization of leupeptin action in the developing rodent conceptus focused on histiotrophic nutrition pathways (HNP) as the principal means through which bulk proteins, specialized carrier proteins, and their essential cargoes (vitamins, minerals, cofactors, growth factors) are captured and processed by the conceptus. With the primary focus on supplying amino acids for protein and nucleic acid biosynthesis, previous studies overlooked the extended developmental consequences of reduced proteolytic activity. It is expected that targeted compartmental disruption of the HNP-dependent nutrient supply pathways could have many other significant effects on the developing embryo. Sant et al. reported that exposure of rat conceptuses in WEC to leupeptin on GD10 and GD11 resulted in significant changes in the concentrations of substrates and cofactors required by the one carbon metabolism pathway (C_1)[10]. S-adenosylmethionine (SAM) concentrations were significantly reduced, as was global DNA methylation in EMB and VYS. These results suggest that disruption of HNP activities along with its subsequent nutritional consequences may be producing acute functional alterations as well as changes in epigenetic programming.

Multiple adverse developmental consequences of altered maternal nutrition during fetal growth have been well documented, with particular emphasis on the roles and functional activities of the placenta [27]. The biochemical and molecular understanding of nutritional fluctuations during early embryogenesis and organogenesis have not been well characterized. Most studies have focused heavily on maternal measurements of nutrient levels in serum. Much less is known about the actual mechanisms of nutrient uptake and utilization in the early embryo during a period that precedes establishment of full functional placental activity. Recent studies suggest that the observed mechanisms of rodent nutrient uptake and processing may also be important in humans during the first trimester [28, 29].

A myriad of molecular switches controlling signaling and regulatory pathways have been studied with respect to their possible roles in directing the complex and overlapping networks of development. None have proven adequate in isolation to describe developmental regulation and control. Widespread recognition of the importance of nutrient

quality and quantity, as well as the roles other environmental regulatory factors, prompt the need to understand the mechanisms behind these signals. Incontrovertible evidence connects the transmission of environmental signals through redox signaling pathways, which are dependent on the regulated synthesis and turnover of soluble thiols such as glutathione (GSH) and cysteine (Cys) and the generation of reactive oxygen species (ROS) as second messengers [30-32]. This work explores the concept that inhibition of HNP activity and the resulting amino acid deficits elicited in the EMB has the potential to influence intracellular redox signaling and alter the thiol proteome as major consequences of HNP inhibition.

MATERIALS AND METHODS

Chemicals and Reagents

Leupeptin hemisulfate salt, FITC-albumin (11.2 mol FITC/mol albumin), glutathione, glutathione disulfide, cysteine, cystine, γ -glutamyl-glutamate, iodoacetic acid, trichloroacetic acid, iodoacetamide, bicinchoninic acid and penicillin/streptomycin (10,000 units/ml penicillin, 10,000 μ g/ml streptomycin sulfate) were purchased from Sigma/Aldrich (St. Louis, MO). Hanks balanced salt solution (HBSS) was purchased from GIBCO/Life Technologies (Grand Island, NY). Dansyl chloride was purchased from Fluka Chemie/Sigma-Aldrich (St. Louis, MO). Cleavable Isotope Coded Affinity Tag (ICAT) reagent kits for protein labeling were purchased from AB Sciex/Applied Biosystems (Framingham, MA). MeOH (HPLC grade) was purchased from Honeywell Burdick & Jackson. All other chemicals were of reagent grade and were purchased from local sources.

Animals

All experiments in this study were conducted using viable, intact GD10 – GD11 conceptuses grown in rat whole embryo culture (WEC). Primagravida specific pathogen free (SPF) Sprague-Dawley rats (Charles River, Portage, MI) were time mated and shipped 4–5 days prior to use. A sperm-positive vaginal smear on the morning following mating was used to confirm pregnancy, this time was designated GD 0. Dams were maintained on a 12 h light–12 h dark cycle and allowed access to standard commercial rodent feed and water *ad libitum*.

Anesthesia, exsanguination, and uteri removal were conducted as previously described and according to an approved institutional animal use and care protocols [33]. Conceptuses were explanted on GD10, prepared for culture and placed into 60-ml culture bottles containing 10 ml of control medium. Two different leupeptin exposure protocols were used, both starting with conceptuses explanted into culture on GD10. The conceptuses in the first protocol, designated as “26 h,” were exposed to 10 μ M, 20 μ M or 50 μ M leupeptin by direct addition to the culture medium on the morning of explant (GD10) and were assessed on GD11 after a total of 26 h in culture. In the second group, designated as “6 h,” conceptuses were cultured for 22 h in control medium from GD10 and then treated with 50 μ M leupeptin on GD11, immediately following the 95% O₂/5% CO₂ gas change, for a total treatment duration of 6 h.

Culture Conditions, Exposure, and Sampling

At the time of explant, gravid uteri were placed in HBSS (pH 7.4 without indicator dyes) and each implantation site was removed using watchmaker's forceps and iridectomy scissors. Decidual masses were opened and intact conceptuses were removed. Reichert's membranes were torn away using fine forceps and the conceptus, consisting of an ectoplacental cone (EPC), intact inverted VYS, amnion, and EMB, were transferred into 10 ml of warmed (37°C) culture medium. A total of 6-10 intact viable conceptuses were placed in the bottles, not to exceed 1 conceptus per ml of medium. Culture medium was prepared from immediately centrifuged, heat inactivated rat serum (50%), HBSS (50%), and 43 μ l penicillin/streptomycin (10,000 U/ml)[33]. Prior to the addition of conceptuses, culture medium and culture bottle headspace were saturated with 20% O₂, 5% CO₂, and 75% N₂, then the medium was warmed to 37 °C. Gestational day 10 embryos at the onset of culture had open anterior neuropores, complete dorsal flexion, and 8–12 somite pairs. Culture occurred in sealed sterile glass bottles on a roller apparatus in a constant 37 °C incubator. After 22 h of culture, the culture medium and headspace were re-saturated with 95% O₂ and 5% CO₂. Leupeptin, dissolved in diH₂O, was added directly to the culture medium at the appropriate times and doses, depending on experimental protocol.

Assessment of Histirotrophic Nutrition Activity

GD11 conceptuses were cultured from GD10 and gassed according to the standard WEC protocol. We have determined in previous experiments that acute perturbations to HNP functions and acute responses to GSH status/redox potential do not differ significantly between GD 10 and GD 11 conceptuses. Because the GD 11 conceptus is approximately 6-10 larger on GD11 and more amenable to experimental manipulation, it is preferentially used for acute exposure experiments [13]. Following gassing and a brief acclimation period, intact conceptuses were transferred to bottles containing 100 mg FITC-albumin/ml of medium. Media was sampled at the beginning of the exposure period and at each sampling time. Acid soluble and TCA insoluble fluorescence were determined for media, VYS, extraembryonic fluids (EEF) and EMB. At each sampling point, conceptuses chosen for analysis were removed from the culture medium and rinsed 3 \times in cold HBSS before being transferred into 50 mM sodium phosphate buffer. Using a pipet tip sized to accommodate the passage of an intact conceptus, the conceptus was placed on a dry petri dish in a 250 μ l drop of buffer. Using watchmaker's forceps, the ectoplacental cone was removed and the VYS and amnion were torn and gently agitated to release EEF into the drop. The VYS was removed, rinsed 3 \times , and placed in 0.1% Triton X-100 on ice. The embryo and amniotic membranes were likewise removed and the remaining drop collected.

All samples were then processed according to the detailed protocol as previously described [13] and acid soluble and acid insoluble fluorescence was determined using a fluorescence plate reader [34]. Relative FITC fluorescence was quantified from a standard curve with instrument settings at 495 nm excitation and 520 nm for emission. Raw fluorescence was converted to a measure of clearance (the volume of media cleared of FITC fluorescence in each compartment per unit time) for VYS, EEF, and EMB, with clearance expressed as μ l/mg protein/hr.

Determination of Thiol Concentrations and Redox Potential

Two tissues sources, VYS and EMB, and two fluid compartments, yolk sac fluid (YSF – the fluid compartment that separates the VYS and the amnion) and amniotic fluid (AF – the fluid compartment found within the amniotic sac and which directly bathes the EMB), were sampled for each GD 11 conceptus from the 26 hr or 6 hr protocols. The 26 hr exposures (GD10-GD11) in rat WEC allow for the onset of exposure at time when the embryo is at an early and very active stage of morphogenesis. The neural tube has just begun to close, the heart has not begun to beat, the embryo is still dorsally rotated. By 26 hr (GD11), the neural tube is almost completely closed and many other structural and functional elements have been established. This time frame allows us to evaluate the effects of chemical exposure on growth, morphogenesis, and functional outcomes. Conceptus dissection and sampling procedures were described elsewhere in detail [35, 36]. Each tissue and fluid was collected in an HPLC preservation buffer containing a final concentration of 5% perchloric acid, 0.2 M boric acid, and 10 10 μM γ -glutamylglutamate [γ -EE] in 300 μl and then snap frozen in liquid nitrogen. Samples can be stored at -74 $^{\circ}\text{C}$ for up to 3 months prior to analysis.

Samples are thawed on ice and prepared for HPLC derivitization using dansyl chloride as described previously according to the methods of Jones [37] and as modified by Harris et al. [36]. Glutathione, GSSG, Cys, and CySS were resolved and quantified using reverse-phase HPLC analysis on a Waters 2695 Alliance Separations Module fitted with a Supelcosil LC-NH₂ column (Sigma-Aldrich, St. Louis, MO). Mobile phases consisted of (A) 80% HPLC grade methanol and 20% ddiH₂O, and (B) 62.5% methanol, 12.5% glacial acetic acid, and 214 mg/ml CH₃COONa-3 H₂O in ddiH₂O with gradient flow at a rate of 1.0 ml/min. Peaks were visualized by fluorescence detection using a Waters 2474 fluorescence detector (excitation 335 nm and emission at 518 nm) and processed with Waters Empower software (Waters, Milford, MA).

Calculations of Cys/CySS and GSH/GSSG E_h are accomplished using the Nernst equation for pH 7.4: GSH/GSSG, $E_h = -264 + 30 \log ([\text{GSSG}]/[\text{GSH}]^2)$, Cys/CySS, $E_h = -250 + 30 \log ([\text{CySS}]/[\text{Cys}]^2)$ and require absolute concentrations for each of the thiol species of interest. Because cell volumes (tissue) and conceptual fluid compartment volumes could not be measured directly, estimations were calculated using two methods. Tissues concentrations for thiols in the VYS and EMB were estimated from total tissue protein using the bicinchoninic acid (BCA) method adapted to the microplate reader [38]. Fluid volumes in the YSF and AF compartments were estimated from average digital measurements of a typical GD 11 conceptus as determined using NIH Image software. Spherical volumes were calculated for the VYS, amnion, and EMB using the equation, $4\pi r^3/3$, and sequentially subtracted to approximate the volume of each compartment.

Sulfhydryl Modification and Analysis of Proteins with Cleavable ICAT Reagents

Samples were obtained from conceptuses cultured from GD10 and treated as above with BSO on GD11 in WEC for 6 h. Conceptuses were harvested from culture and processed for ICAT analysis as described elsewhere [33] and [34] and with accordance to the manufacturer's instructions (AB Sciex/Applied Biosystems). In brief, 100 μg of untreated control EMB and 100 μg of BSO-treated EMB tissues were labeled with the maleimide

ICAT reagents (Light ^{12}C isotope for untreated controls and ^{13}C Heavy isotope for the BSO-treated test samples, thus, providing a direct comparison of relative protein abundance between treated and control samples. Protein samples were prepared for mass spectrometry analysis per instructions provided by the manufacturer (AB Sciex/Applied Biosystems), allowing for fragmentation analysis of labeled proteins. The labeled and digested peptides were subjected to strong cation exchange chromatography (SCX). A Dionex U-3000 capillary HPLC equipped with a capillary pump and a microbore pump were used for the analysis. The microbore pump was used to generate a linear gradient for the SCX separation. The samples were reconstituted in the starting buffer of 5 mM KH_2PO_4 (pH 3)/5% acetonitrile (ACN). An aliquot was injected onto a SCX column (Polysulfoethyl-Asp, 1×15 cm, Dionex). The peptides were eluted off the SCX column using a linear gradient of 0–100% 1 M NaCl/5% ACN/5 mM KH_2PO_4 over 20 min at a flow rate of 50 $\mu\text{l}/\text{min}$. The eluent was collected by time into 10–14 fractions. An aliquot of each fraction was then analyzed by RP-HPLC on the maXis LC-MS/MS system as described below. Electrospray ionization (ESI) mass spectrometric analysis was performed using a Bruker Model maXis ESI-Q-TOF instrument interfaced with an on-line nanospray source (Bruker Daltonics) to perform LC-MS/MS using a U3000 RSLCnano HPLC, configured for nanoliter per minute flows. Complete analytical details were described previously [35].

The principle output from an ICAT analysis following trypsin digestion and resolution by mass spectroscopy was the H/L ratio (Heavy/Light). Only H/L ratios that deviated from unity by more than 25% were considered significantly different and included in subsequent analysis. Proteins meeting these criteria were interrogated using the Kyoto Encyclopedia of Genes and Genomes (KEGG) pathway database (<http://www.genome.jp/kegg>) to predict functional pathway associations and links among proteins. Only proteins for which KEGG had available pathway data and met the significant change criteria were included for the purposes of this study. Rigorous statistical analysis applied to pathway criteria identified pathways that were significantly altered by leupeptin treatment. Individual proteins not associated with significantly altered pathways, but changed due to leupeptin treatment, were listed in figures and supplemental tables, grouped by pathway and function.

Statistical Analysis

Tabular values listed in tables and figures are generally shown as mean values without the \pm standard error of the mean (SEM) shown in order to allow better clarity for presentation of the results. Statistical outliers were removed after meeting the criteria of 1.5 times the interquartile range from each measure. ANOVA with Tukey's post hoc tests and Student's *t* tests were used for statistical comparisons. A confidence level of 95% ($\alpha=0.05$) was used as threshold for statistical significance.

RESULTS

The two protocols used for leupeptin treatment in WEC allows for assessment of exposure outcomes over a 26 hr period from GD10 to GD11 and more acutely on GD11 over a short 1, 3, and 6 hr time course. The 26 hr paradigm allows for an accurate assessment of effects on overall growth, morphogenesis, and cumulative changes in biochemical parameters. The

acute time course on GD11 corresponds with optimal stages for assessment of HNP activity and other biochemical and molecular events that occur during the first 6 hr after exposure, including redox changes and alterations to the thiol proteome.

Redox Profiles

26 hr Leupeptin Exposure (GD10 – GD11)—Changes in GSH/GSSG and Cys/CySS status were assessed in tissues (VYS and EMB) and fluid compartments (YSF and AF) of GD11 conceptuses after 26 hr in WEC. The direct addition of leupeptin to culture media on GD 10 at concentrations of 10 μ M and 20 μ M resulted in depletion of total GSH (GSH + 2GSSG) in the VYS by 78% and 82% respectively. During the same period, no significant reductions in total GSH were observed in the EMB proper (Figure 1). Ratios of GSSG/GSH remained fairly constant within the significantly depleted VYS following leupeptin, but increased significantly in the EMB during the same period. Total GSH was only marginally and dose-dependently depleted in the YSF and AF compartments after 26 hr.

Leupeptin inhibition of proteolytic activity in the VYS resulted in a net dose-dependent increase in total Cys (Cys + 2CySS) of nearly 60% at 10 μ M leupeptin in the VYS, but was accompanied by a significant increase in the CySS/Cys ratio. In the EMB, 10 μ M leupeptin produced a modest elevation in total Cys and CySS/Cys ratio, while levels were unchanged at 20 μ M. In the fluid compartments, total Cys was decreased in YSF and AF without much relative change in CySS/Cys ratios as absolute Cys concentrations alone did not change significantly.

Based on the absolute estimated concentrations of oxidized and reduced GSH and Cyss, redox potentials (E_h) were calculated for tissues and fluid compartments following 26 hr leupeptin exposure (Figure 2). Data from 10 μ M and 20 μ M leupeptin doses are shown, as well as a 50 μ M leupeptin dose, extracted from previous experiments, for comparison. Redox potentials for the GSSG/GSH couple in the VYS show a dose-dependent increase (oxidation) with increasing concentrations of leupeptin, reaching optimal 36 mV and 37 mV increases for 20 μ M and 50 μ M leupeptin, respectively. A greater magnitude of oxidation was seen in the embryo proper where optimal changes of 60 mV were seen with 20 μ M leupeptin as E_h increased to -146 mV. E_h fluctuations in the fluid compartments were less pronounced, not to exceed 18 mV in the YSF, with very little change in the AF. For the CySS/Cys redox couple, E_h became more positive in the VYS, reaching an optimal change of 22 mV with 20 μ M leupeptin. YSF and AF fluctuated within a narrow range of around 15 mV while the tissues of the EMB actually became more negative (reduced) by an optimal 50 mV with 20 μ M leupeptin (Figure 2).

Inhibition of Proteolysis and Assessment of HNP Activity

The results shown in Figure 3 verify the ability of leupeptin to reduce total clearance of FITC-albumin from culture media into the conceptus at concentrations as low as 10 μ M. After a 3 hr pulse with FITC-albumin in the untreated conceptus, over 80% of the total cleared FITC label was found in the VYS, nearly equally distributed between the soluble and insoluble forms. Protease inhibition with leupeptin reduced the soluble fluorescence by greater than 90%, leaving only the insoluble (undegraded) protein. As expected, extra

embryonic fluids (YSF and AF), contained much smaller amounts of FITC fluorescence, mostly in the soluble form. Very little fluorescence reaches the EMB proper [13]. Optimal decreases in total clearance of 33% and 44% were seen at 10 μ M and 20 μ M leupeptin on GD11 respectively after exposure for 26 hr and were not further decreased at higher doses. These results confirmed previous studies which showed the HNP inhibitory effects of leupeptin on the protease component of the nutritive activity [4, 13].

6 hr Time Course on GD 11 – 50 mM Leupeptin—Short-term time course redox profile data for VYS and EMB tissues was generated to allow a direct correlation of soluble thiol concentrations, redox potentials (E_h), alterations to the thiol proteome and concurrent changes in HNP activity. Comparisons to concurrent controls at each time point showed only slight reductions in total VYS GSH at 1hr, 3hr, and 6hr following leupeptin exposure (Figure 4). Although changes in total GSH were not significant, they did result in significant E_h increases of 20 mV and 18 mV at 3hr and 6hr, respectively, due to disproportionate increases in GSSG concentrations. Similar patterns were seen for the CySS/Cys redox couple where total Cys showed no significant decreases at all time points relative to concurrent controls. E_h values increased proportional to dose by 49 mV and 51 mV at 3hr and 6hr respectively.

In the EMB, total GSH was also decreased as a result of leupeptin exposure, but to a much lesser degree when compared to the VYS. Total GSH decreased by 15% to 26% over 6hr and total Cys decreased by 36% during the same period. These changes translate to positive shifts in E_h for both redox couples which were optimal at 13 mV for GSSG/GSH and 45 mV for CySS/Cys at the 6hr time point. In order for these changes to occur, GSSG/GSH and CySS/Cys ratios increased dramatically in exposed tissues. Much like the 26hr exposure, leupeptin elicited a significant depletion of the soluble thiols GSH and Cys and caused an acute net oxidation of conceptual tissues (Figure 4).

Thiol Proteomics—Labeling of protein thiols with cleavable ICAT reagents provided a comparative assessment of changes to the thiol proteome in EMB and VYS following 6 hr of leupeptin (50 mM) exposure on GD 11. The exposure period covered in this protocol was identical to the 6 hr GD 11 time course reported for determination of redox profiles and is similar to the timing of the HNP activity determination. Ratios of heavy/light stable isotopic ($^{13}\text{C}/^{12}\text{C}$) labeling for each protein identified dictate the extent to which the protein is increased (H/L ratio $>$) or decreased (H/L ratio <1) due to leupeptin treatment. Of the 41 most abundant proteins identified in the VYS, only 9 were decreased in concentration while all others increased (Figure 5). In the EMB proper, a total of 97 proteins were identified by mass spectroscopy, only three of which were increased in concentration as a result of treatment. This shows a definite pattern of overall protein decrease in the EMB, alongside predominant increases and lesser-mixed changes in the VYS. KEGG pathway analysis of the proteomic data shows few clear disruptions in multiple specific pathways but, rather, more general alterations. **Glycolysis/gluconeogenesis** was the pathway most affected by leupeptin in the VYS. In the EMB the only significant pathway to emerge was for **ribosomes**, but included a total of 38 different proteins involved in ribosome biogenesis, assembly and activity. Only 12 of the specific proteins that changed as a result of leupeptin exposure were

common to both EMB and VYS (Figure 5). These included heat shock proteins, cytoskeleton-related, carbohydrate metabolism, and ribosome-related proteins.

Of particular note are the 16 most increased proteins identified in the VYS. These proteins increased in concentration from 2.2-fold to 21.6 fold by the end of the exposure period and are all known to be common serum/blood proteins (Figure 6) (Supplemental Table S1). These are the proteins captured by RME activity at the VYS brush border, but which are not degraded to their constitutive amino acids due to the effective protease inhibition of leupeptin (Figure 6). Serum albumin and alpha-fetoprotein were the only two serum-related proteins that were also found in EMB and both were of the small subset in the EMB that were increased in concentration. Complete lists of proteins altered as a result of protease inhibition in organogenesis-stage rat conceptuses are found in Supplementary Table S1.

Specific endogenous proteins altered in the VYS (captured serum proteins excluded) included several enzymes involved in carbohydrate metabolism (KEGG Glycolysis/Gluconeogenesis) such as the aldolases, enolases, and pyruvate kinases (Table S1). In addition, the concentrations of several heat shock proteins, cytoskeletal proteins (actin, tubulin, and related regulatory elements), lysosomal cysteine proteases (cathepsins B and Z), and ribosome associated proteins were affected by leupeptin treatment in the VYS. In the EMB, a total of 14 proteins mapped significantly to the KEGG Ribosome Pathway. Grouping these specific proteins with others associated with the broader activities of ribosome biogenesis, ribosome assembly, and translation activity, this group includes at least 39 of the top proteins decreased in concentration due to leupeptin treatment (Table S2). Other decreases in the EMB include proteins associated with cytoskeleton and vesicular transport, carbohydrate and intermediary metabolism, heat shock proteins, and some specific carrier and binding proteins (cellular retinoic acid-binding protein, fatty acid binding protein – epidermal).

DISCUSSION

The organogenesis stage rodent conceptus relies almost exclusively on the dual VYS functions of receptor-mediated endocytosis (RME) and lysosomal proteolysis to capture whole maternal proteins and then degrade them to free amino acids in order to provide for all of the biosynthesis needs of the developing EMB. Receptor mediated endocytosis and lysosomal proteolysis are the key integrated activities of histiotrophic nutrition pathways (HNP) that capture and import bulk proteins as the source of substrate amino acids and other carrier proteins, along with their cargoes of vitamins, cofactors, lipids, minerals, growth factors, and other critical micronutrients that make up the majority of required EMB nutrients [7, 8]. The majority of previous HNP studies have been focused on the organogenesis period of development and have primarily considered the supply of amino acid precursors exclusively for protein and nucleotide biosynthesis [39] [1, 3, 6, 28, 29]. More recent studies have turned attention to understanding the possible signaling and regulatory consequences of partial or complete inhibition of EMB nutrient uptake and processing. We have previously reported that the natural protease inhibitor, leupeptin, decreases the availability of substrates and cofactors required by one carbon metabolism (C_1), and results in the decreased availability of S-adenosylmethionine (SAM), the universal

methyl donor required for DNA and histone protein methylation in epigenetic programming. As a result of protease inhibition by leupeptin, global DNA methylation was significantly decreased in both VYS and EMB [10]. Still unknown are the precise mechanisms through which these changes are wrought and how specific changes in regulatory and signaling pathways affect a wide variety of developmental outcomes (Figure 5).

The overall inhibition of HNP, based on measured clearance of FITC-albumin from the culture medium (Figure 3), shows that leupeptin treatment causes a significant reduction in acid-soluble fluorescence, indicating the lost ability to degrade captured proteins to their constituent acid-soluble amino acids. The significant accumulation of “serum” proteins in the VYS following protease inhibition in WEC confirms the source of nutrient proteins (serum in culture medium) and the importance of their quantity and quality as a nutrient source under these experimental conditions. (Table S1)(Figure 6). A 6 hr exposure to leupeptin (50 μM) on GD 11 results in a 79% increase in total VYS protein, relative to concurrent controls [10], and correlates with the observed 2-22 fold increases in specific individual serum proteins identified in the proteomic (ICAT) analysis (Figure 5).

In addition to the obvious nutritional consequences of amino acid starvation, protease inhibition also elicits significant effects related to redox regulation and control in the developing conceptus. The dynamic process of GSH biosynthesis is largely responsible for maintaining a proper redox environment for growth and differentiation in the conceptus during organogenesis. The VYS is the primary site of GSH biosynthesis and is believed to actively export GSH to provide amino acid precursors to the EMB proper for its GSH synthesis needs [40]. Reduction of precursor amino acid availability through protease inhibition severely limits GSH biosynthesis as seen by the significant drop in total GSH in the VYS (Figure 1). In this study, reduced and total GSH were significantly depleted during an exposure of 6 hr (50 μM leupeptin; Figure 4) on GD11 and were even more significantly depleted over a 26 hr exposure at leupeptin concentrations of 10 μM or 20 μM (Figure 1). Total Cys concentrations followed those for total GSH in the 6h exposure group, but showed a much different pattern after 26 hr (GD10 – GD11). At 26 hr, total Cys concentrations in both VYS and EMB were unexpectedly increased following leupeptin exposure. The observed increases in total Cys are almost exclusively due to elevated CySS because the absolute concentrations of Cys changed very little as a function of time or leupeptin dose. Under normal conditions, excess Cys would be expected to facilitate increased GSH biosynthesis, but we observed that total GSH concentrations are significantly reduced in combination with the large increase in total Cys. In cases of general amino acid starvation, it is possible that deficiencies in the other GSH precursor amino acids, Gly and Glu, a lack of ATP required for biosynthesis, or the loss of anabolic enzymes are contributing to a lack of GSH biosynthesis.

The ability of the developing conceptus to maintain and regulate adequate concentrations of GSH has been shown to impact several aspects of growth and differentiation in the conceptus [31, 41]. Measured increases in total GSH and Cys concentrations or a lack of significant concentration change in conceptual compartments might suggest minimal effects of leupeptin on the redox environment based on contemporary definitions of oxidative stress. However, using redox potentials calculated from direct measurements of GSSG/GSH

and CySS/Cys redox couples as a readout of perturbations to the redox steady state, these metrics provide a more accurate correlate with induced shifts in redox signaling and alterations to transcriptional activation pathways [36, 41]. Under the conditions of amino acid starvation reported in this study, leupeptin produced redox potential increases (net oxidation) in VYS and EMB during 6hr and 26 hr exposures. Of particular interest was the substantial reduction of total GSH concentrations in the VYS (Figure 1) after 26 hr, accompanied by moderate but significant increases in redox potential (+36 mV), and the corresponding small decrease in total GSH in the EMB accompanied by a highly significant +60 mV oxidation in the EMB (Figure 2). This result suggests that the EMB, unlike the VYS, is able to preserve total GSH concentrations during protease inhibition but is unable to maintain GSH in a reduced state. In contrast, redox potentials for the CySS/Cys redox couple show dose-dependent oxidations like the GSSG/GSH couples in the VYS but trend toward higher variability and increased reducing conditions in the EMB. The precise mechanisms of these processes are currently unknown but imply an important role for selective compartmental regulation and activation of adaptive responses that work together to preserve EMB function and viability. Several direct consequences of altered redox state have been reported in conceptuses including the misregulation of Nf- κ B, AP-1, and Mat2a [42-44] and the regulation of protective responses through Nrf-2 [31, 45]. No other systematic reports have been found to describe altered redox signaling during embryogenesis caused by alterations in nutrient availability or processing.

The continued accumulation of proteins in the VYS resulting from protease inhibition decreases amino acid availability in the whole conceptus, creating conditions akin to the amino acid starvation that has been described for yeast and other experimental models [46]. Cellular adaptation to amino acid starvation includes attempts to adjust intracellular conditions toward reduced energy demand through decreased macromolecule synthesis, increased macromolecule turnover, altered active ion flux, and the increased removal of damaged or potentially harmful cellular proteins and products via autophagy. Even while limiting the thiol proteomic analysis to the 2.5% of most abundant proteins, several conclusions can be drawn from these results. The major changes seen in the proteomic profiles and affected pathways for EMB and VYS following leupeptin exposure are consistent with expected responses to amino acid starvation and are distinctively compartmental in nature. From an energy perspective, the only significant pathway changed in the VYS after rigorous selection was for an increase in protein concentrations associated with glycolysis and gluconeogenesis pathways that include proteins such as the enolases, aldolases and phosphatases (Supplemental Table 1.). The conceptus relies heavily on this pathway during organogenesis for meeting its energy demands due to an immature Krebs cycle activity that is present prior to initiation of the heartbeat and activation of oxygen and nutrient circulation [47]. Increased glycolytic activity is expected to be essential for conceptual survival. In the VYS, of the 60 endogenous proteins evaluated in this study, 44 were found to have an H/L ratio change greater than 0.15. Of these, 34 proteins were found to be increased in concentration. This is in contrast to the EMB proper where 98 of 105 proteins were changed and all but three of the changes were decreases in concentration. The compartmental nature of responses to leupeptin exposure is shown in Figure 5 even for differentially altered proteins that were common to VYS and EMB.

Reductions in rates of protein biosynthesis occur rapidly when amino acids are limiting and the low residual rates that remain are believed to be augmented by using precursors made available from autophagy. Changes in the rates of protein synthesis when amino acids are limited are also regulated through a coordinated interplay with alterations in mitochondrial energy production [48]. Biosynthesis of the ribosomes and subsequent protein synthesis are considered to be the most energy-consuming process in the cell, where over 80 ribosomal proteins, 4 rRNAs, and up to 200 other different proteins are responsible for creating an intact and functionally mature ribosome and maintenance of this super-system requires greater than three quarters of all cellular energy to maintain [49, 50]. In addition to the extensive reported decreases in the abundance of ribosomal proteins themselves, our proteomic analyses have also identified changes in proteins required for nuclear import/export, RNA transcription, protein assembly, and processing of proteins (Figure 6; Supplemental Tables 1, 2). The observed decreases in heat shock, chaperone, and related proteins in the EMB and VYS also suggest that cells in the conceptus switch from protein preservation to active reduction of total nonessential protein concentrations. Heat shock and related proteins are responsible for protecting proteins from denaturation and degradation and are found to decrease in both VYS and EMB following leupeptin. This is also consistent with adaptation to amino acid starvation because the cells under these conditions are actively degrading all excess proteins to conserve energy.

The primary objective of this work was to examine the potential regulatory and functional changes that occur during rat organogenesis when specific histiotrophic nutrition functions are altered. While most investigations of HNP have focused on deficiencies in protein and nucleic acid synthesis that occur when amino acid precursors are depleted, this report shows that induced alterations in several other critical pathways, processes, and signaling functions may be contributing to mechanisms of developmental toxicity and teratogenicity. Developmental implications for altered conceptual nutrition range from the regulation of growth, along with acute protective and adaptive responses, to the epigenetic reprogramming events that exert regulatory control across the entire lifespan and into subsequent generations. Based on the proteomic analysis, the immediate consequences of protease inhibition with leupeptin are manifest as amino acid starvation with a dramatic deregulation of ribosome biogenesis, ribosome structure and function, elimination of excess proteins, and adjustments in metabolism and energy utilization characteristic of cononical pathways of autophagy. Regulation of autophagy had been shown to be important during mammalian development [51, 52]. Concurrent consequences of amino acid depletion also include the compartmental attenuation of GSH biosynthesis, which has the result of oxidizing cellular environments and altering developmentally critical redox signaling pathways. Previous studies have suggested that many known teratogens act through the generation of excess ROS and consequences may be mediated through mechanisms where susceptibility to chemical toxicants is influenced by availability of adequate nutrients [16] [41]. What has not been systematically explored is the association between redox status and the activation and regulation of autophagy during development. Autophagy is an extensively redox-regulated process, dependent on specific thiol switches at almost every stage of regulation [53-55] The inhibition of HNP activities in the VYS of developing conceptuses are shown to alter compartmental redox states, and cause dramatic changes to the thiol

proteome. Future investigations should consider the disruption of conceptual nutritional pathways as a sensitive common target for chemical and environmental insults that negatively impact developmental growth, differentiation, and morphogenesis.

Supplementary Material

Refer to Web version on PubMed Central for supplementary material.

REFERENCES CITED

- [1]. Freeman SJ, Lloyd JB. Evidence that protein ingested by the rat visceral yolk sac yields amino acids for synthesis of embryonic protein. *Journal of Embryology and Experimental Morphology*. 1983; 73:307–315. [PubMed: 6875463]
- [2]. Brent RL. Nutritional studies of the embryo during early organogenesis with normal embryos and embryos exhibiting yolk sac dysfunction. *The Journal of pediatrics*. 1998; 132:S6–16. [PubMed: 9546031]
- [3]. Beckman DA. Investigations into mechanisms of amino acid supply to the rat embryo using whole-embryo culture. *The International journal of developmental biology*. 1997; 41:315–318. [PubMed: 9184340]
- [4]. Beckman DA. Sources of amino acids for protein synthesis during early organogenesis in the rat. I. Relative contributions of free amino acids and of proteins. *Placenta (Eastbourne)*. 1990; 11:109–121.
- [5]. Beckman DA, Pugarelli JE, Koszalka TR, Brent RL, Lloyd JB. Sources of amino acids for protein synthesis during early organogenesis in the rat. 2. Exchange with amino acid and protein pools in embryo and yolk sac. *Placenta*. 1991; 12:37–46. [PubMed: 2034594]
- [6]. Beckman DA, Brent RL, Lloyd JB. Sources of amino acids for protein synthesis during early organogenesis in the rat. 4. Mechanisms before envelopment of the embryo by the yolk sac. *Placenta*. 1996; 17:635–641. [PubMed: 8916213]
- [7]. Moestrup SK. Megalin- and cubilin-mediated endocytosis of protein-bound vitamins, lipids, and hormones in polarized epithelia. *Annual review of nutrition*. 2001; 21:407–428.
- [8]. Assémat E, Vinot S, Gofflot F, Linsel-Nitschke P, Illien F, Châtelet F, Verroust P, Louvet-Vallée S, Rinninger F, Kozyraki R. Expression and Role of Cubilin in the Internalization of Nutrients During the Peri-Implantation Development of the Rodent Embryo. *Biology of Reproduction*. 2005; 72:1079–1086. [PubMed: 15616221]
- [9]. Kozyraki R. Multiligand endocytosis and congenital defects: roles of cubilin, megalin and amnionless. *Current pharmaceutical design*. 2007; 13:3038–3046. [PubMed: 17979745]
- [10]. Sant KE, Dolinoy DC, Nahar MS, Harris C. Inhibition of proteolysis in histiotrophic nutrition pathways alters DNA methylation and one-carbon metabolism in the organogenesis-stage rat conceptus. *The Journal of Nutritional Biochemistry*. 2013; 24:1479–1487. [PubMed: 23453262]
- [11]. Beckman DA. Quantitative studies on the mechanisms of amino acid supply to rat embryos during organogenesis. *Reproductive toxicology (Elmsford, N.Y.)*. 1998; 12:197–200.
- [12]. Ambroso JL, Harris C. In vitro embryotoxicity of the cysteine proteinase inhibitors benzyloxycarbonyl-phenylalanine-alanine-diazomethane (Z-Phe-Ala-CHN₂) and benzyloxycarbonyl-phenylalanine-phenylalanine-diazomethane (Z-Phe-Phe-CHN₂). *Teratology*. 1994; 50:214–228. [PubMed: 7871486]
- [13]. Ambroso JL, Larsen SV, Brabec RK, Harris C. Fluorometric analysis of endocytosis and lysosomal proteolysis in the rat visceral yolk sac during whole embryo culture. *Teratology*. 1997; 56:201–209. [PubMed: 9358607]
- [14]. Ambroso JL. Chloroquine embryotoxicity in the postimplantation rat conceptus in vitro. *Teratology (Philadelphia)*. 1993; 48:213–226.
- [15]. Steventon GB, Williams KE. Ethanol-induced inhibition of pinocytosis and proteolysis in rat yolk sac in vitro. *Development*. 1987; 99:247–253. [PubMed: 3653000]

- [16]. Jilek JL, Sant KE, Cho KH, Reed MS, Pohl J, Hansen JM, Harris C. Ethanol Attenuates Histiotrophic Nutrition Pathways and Alters the Intracellular Redox Environment and Thiol Proteome during Rat Organogenesis. *Toxicological Sciences*. 2015
- [17]. Freeman SJ. Inhibition of proteolysis in rat yolk sac as a cause of teratogenesis. Effects of leupeptin in vitro and in vivo. *Journal of Embryology and Experimental Morphology*. 1983; 78:183–193. [PubMed: 6663224]
- [18]. Knowles SE. Effects of microbial proteinase inhibitors on the degradation of endogenous and internalized proteins by rat yolk sacs. *Biochemical journal*. 1981; 196:41–48. [PubMed: 7306078]
- [19]. Maeda K. The structure and activity of leupeptins and related analogs. *Journal of antibiotics*. 1971; 24:402–404. [PubMed: 4253693]
- [20]. Aoyagi T. Leupeptins, new protease inhibitors from Actinomycetes. *Journal of antibiotics*. 1969; 22:283–286. [PubMed: 5810993]
- [21]. Gavriel H. Leupeptin reduces impulse noise induced hearing loss. *Journal of occupational medicine and toxicology (London, England)*. 2011; 6:38.
- [22]. Momiyama J. Leupeptin, a calpain inhibitor, protects inner ear hair cells from aminoglycoside ototoxicity. *Tohoku journal of experimental medicine*. 2006; 209:89–97. [PubMed: 16707850]
- [23]. Rosenthal PJ. A malarial cysteine proteinase is necessary for hemoglobin degradation by *Plasmodium falciparum*. *The Journal of clinical investigation*. 1988; 82:1560–1566. [PubMed: 3053784]
- [24]. Tözsér J. Proteolytic events of HIV-1 replication as targets for therapeutic intervention. *Current pharmaceutical design*. 2003; 9:1803–1815. [PubMed: 12871198]
- [25]. Kourjian G. Sequence-Specific Alterations of Epitope Production by HIV Protease Inhibitors. *The Journal of immunology*. 2014 1950.
- [26]. Quan GB, Han Y, Yang C, Hu WB, Liu A, Wang JX, Wang Y, Liu MX. Inhibition of high glucose-induced erythrocyte phosphatidylserine exposure by leupeptin and disaccharides. *Cryobiology*. 2008; 56:53–61. [PubMed: 18093577]
- [27]. Bloomfield FH. Nutritional regulation of fetal growth. *Nestlé Nutrition Institute Workshop Series*. 2013; 74:79–89. [PubMed: 23887106]
- [28]. Burton GJ. Nutrition of the human fetus during the first trimester--a review. *Placenta (Eastbourne)*. 2001; 22(Suppl A):S70–77.
- [29]. Burton GJ. Uterine glands provide histiotrophic nutrition for the human fetus during the first trimester of pregnancy. *The journal of clinical endocrinology and metabolism*. 2002; 87:2954–2959. [PubMed: 12050279]
- [30]. Finkel T. Signal transduction by reactive oxygen species. *The Journal of Cell Biology*. 2011; 194:7–15. [PubMed: 21746850]
- [31]. Hansen JM, Harris C. Redox control of teratogenesis. *Reproductive Toxicology*. 2013; 35:165–179. [PubMed: 23089153]
- [32]. Takahashi M. Oxidative Stress and Redox Regulation on *In Vitro* Development of Mammalian Embryos. *Journal of Reproduction and Development*. 2012; 58:1–9. [PubMed: 22450278]
- [33]. Harris C. Rodent whole embryo culture. *Methods in molecular biology (Clifton, N.J.)*. 2012; 889:215–237.
- [34]. Ambroso, J.; Harris, C. Assessment of Histiotrophic Nutrition Using Fluorescent Probes. In: Harris, C.; Hansen, JM., editors. *Developmental Toxicology*. Vol. 889. Humana Press; 2012. p. 407–423.
- [35]. Harris C, Shuster DZ, Roman Gomez R, Sant KE, Reed MS, Pohl J, Hansen JM. Inhibition of glutathione biosynthesis alters compartmental redox status and the thiol proteome in organogenesis-stage rat conceptuses. *Free Radical Biology and Medicine*. 2013; 63:325–337. [PubMed: 23736079]
- [36]. Harris C. Oxidative stress, thiols, and redox profiles. *Methods in molecular biology (Clifton, N.J.)*. 2012; 889:325–346.

- [37]. Jones, DP. [11] Redox potential of GSH/GSSG couple: Assay and biological significance. In: Helmut, S.; Lester, P., editors. *Methods in Enzymology*. Vol. 348. Academic Press; 2002. p. 93-112.
- [38]. Kirlin WG. Glutathione redox potential in response to differentiation and enzyme inducers. *Free radical biology & medicine*. 1999; 27:1208–1218. [PubMed: 10641713]
- [39]. Rowe PB, Kalaizis A. Serine metabolism in rat embryos undergoing organogenesis. *Journal of embryology and experimental morphology*. 1985; 87:137–144. [PubMed: 2411839]
- [40]. Harris C. Glutathione Biosynthesis in the Postimplantation Rat Conceptus in Vitro. *Toxicology and Applied Pharmacology*. 1993; 120:247–256. [PubMed: 8511794]
- [41]. Hansen JM, Harris C. Glutathione during embryonic development. *Biochimica et Biophysica Acta (BBA) - General Subjects*. 2015; 1850:1527–1542.
- [42]. Hansen JM. A novel hypothesis for thalidomide-induced limb teratogenesis: redox misregulation of the NF-kappaB pathway. *Antioxidants & redox signaling*. 2004; 6:1–14. [PubMed: 14713331]
- [43]. Ozolinš TRS. Regulation and control of AP-1 binding activity in embryotoxicity. *Methods in molecular biology (Clifton, N.J.)*. 2012; 889:291–303.
- [44]. D. DC, Sant KS, Nahar MS, Harris C. Histiotrophic nutrition informs DNA methylation in the rat conceptus. *Journal of Nutritional Biochemistry*. 2013 In Press.
- [45]. Harris C, Hansen JM. Nrf2-Mediated Resistance to Oxidant-Induced Redox Disruption in Embryos. *Birth Defects Research Part B: Developmental and Reproductive Toxicology*. 2012; 95:213–218.
- [46]. Grummt I, Smith VA, Grummt F. Amino acid starvation affects the initiation frequency of nucleolar RNA polymerase. *Cell*. 1976; 7:439–445. [PubMed: 947551]
- [47]. Hunter, ES, III. Interference with Embryonic Intermediary Metabolism. In: Kavlock, R.; Daston, G., editors. *Drug Toxicity in Embryonic Development I*. Vol. 124 / 1. Springer; Berlin Heidelberg: 1997. p. 373-406.
- [48]. Johnson MA. Amino Acid starvation has opposite effects on mitochondrial and cytosolic protein synthesis. *PloS one*. 2014; 9:e93597. [PubMed: 24718614]
- [49]. Henras AK, Soudet J, G erus M, Lebaron S, Caizergues-Ferrer M, Mougou A, Henry Y. The post-transcriptional steps of eukaryotic ribosome biogenesis. *Cell. Mol. Life Sci*. 2008; 65:2334–2359. [PubMed: 18408888]
- [50]. Fromont-Racine M, Senger B, Saveanu C, Fasiolo F. Ribosome assembly in eukaryotes. *Gene*. 2003; 313:17–42. [PubMed: 12957375]
- [51]. Aburto MR, Hurl e JM, Varela-Nieto I, Magari nos M. Autophagy During Vertebrate Development. *Cells*. 2012; 1:428–448. [PubMed: 24710484]
- [52]. Cecconi F, Levine B. The Role of Autophagy in Mammalian Development: Cell Makeover Rather than Cell Death. *Developmental Cell*. 2008; 15:344–357. [PubMed: 18804433]
- [53]. Cardaci S, Filomeni G, Ciriolo MR. Redox implications of AMPK-mediated signal transduction beyond energetic clues. *Journal of Cell Science*. 2012; 125:2115–2125. [PubMed: 22619229]
- [54]. Filomeni G, De Zio D, Cecconi F. Oxidative stress and autophagy: the clash between damage and metabolic needs. *Cell Death Differ*. 2014
- [55]. Scherz-Shouval R, Shvets E, Fass E, Shorer H, Gil L, Elazar Z. Reactive oxygen species are essential for autophagy and specifically regulate the activity of Atg4. *The EMBO Journal*. 2007; 26:1749–1760. [PubMed: 17347651]

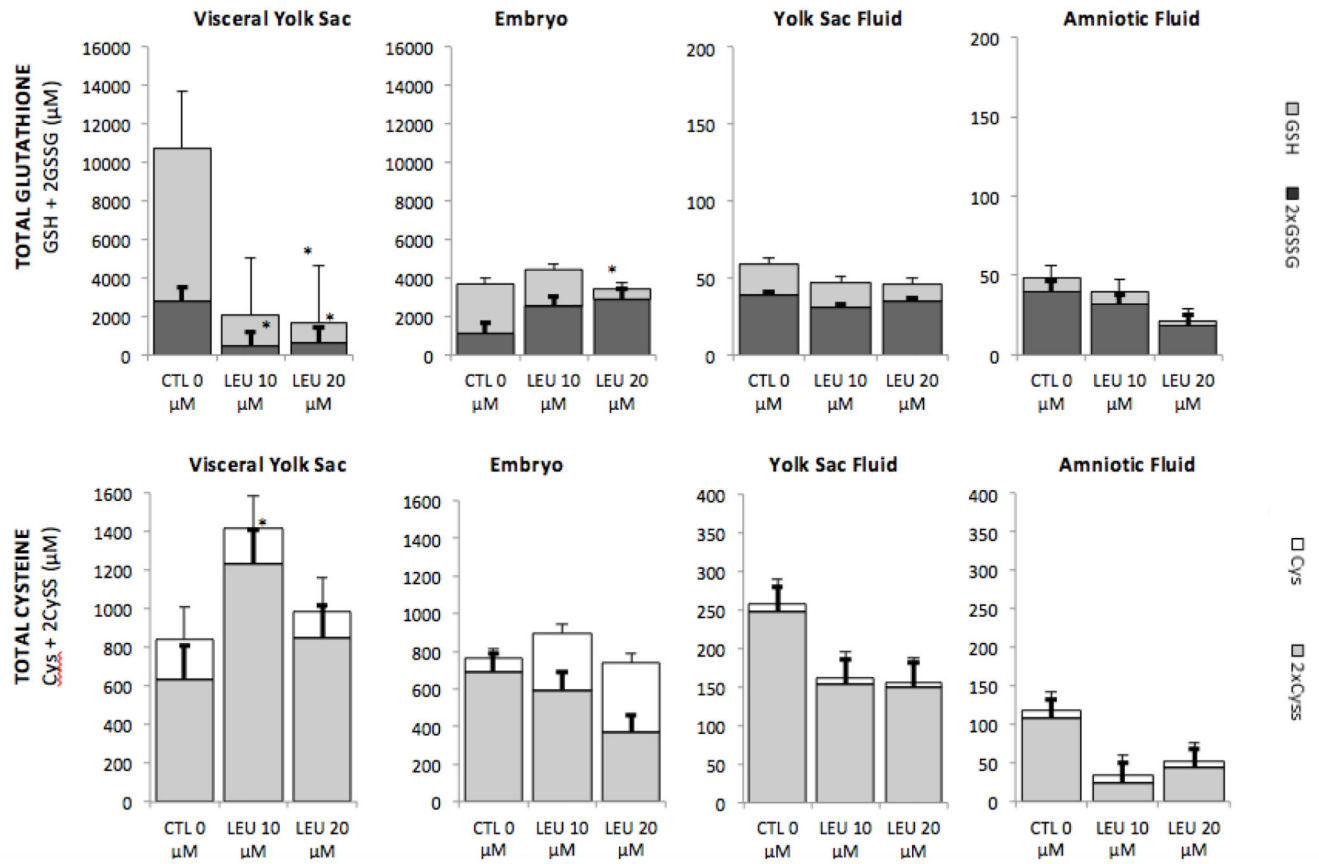
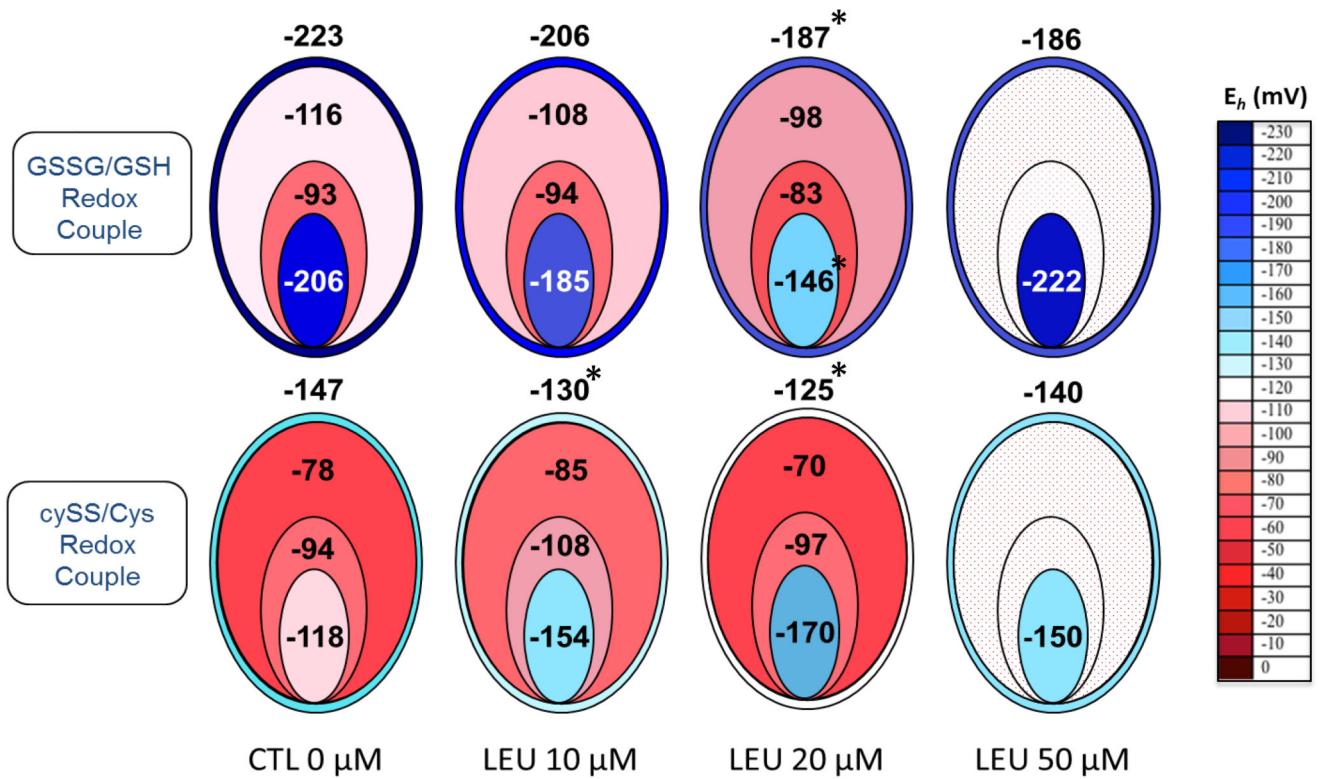
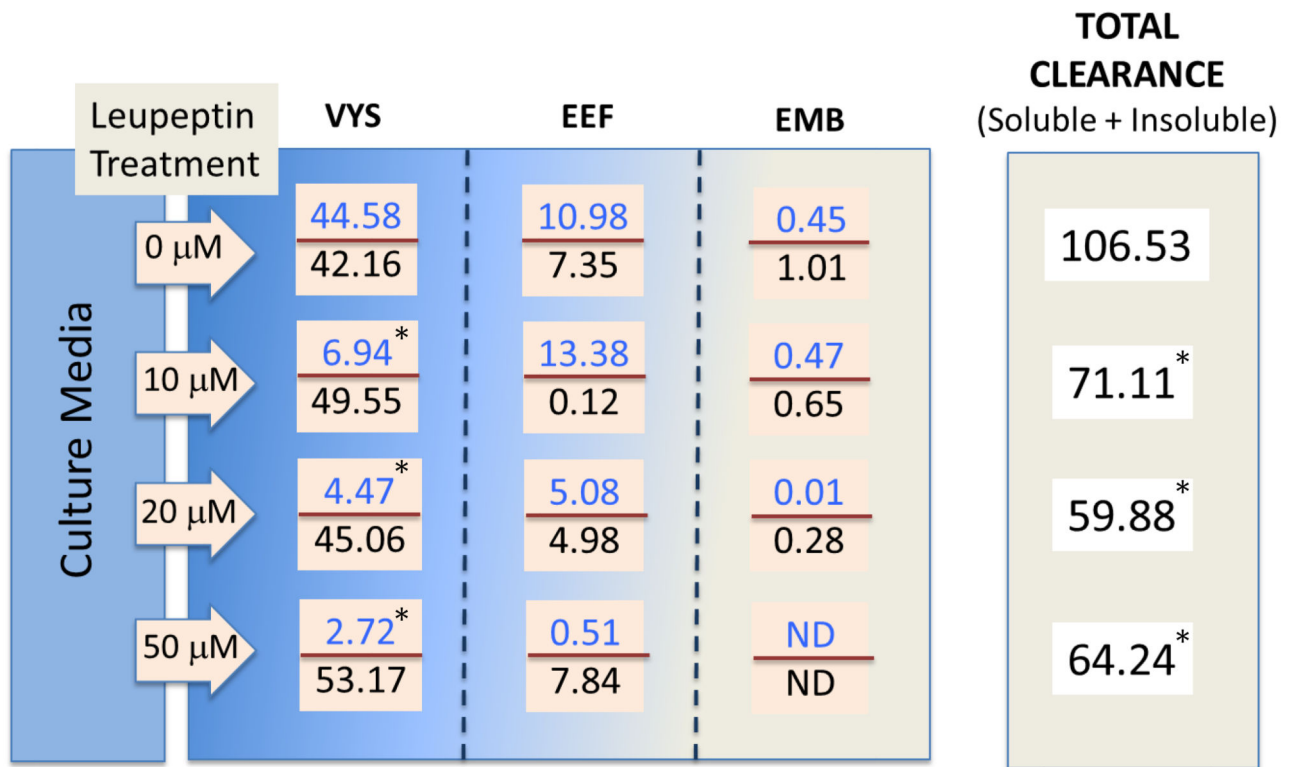


FIGURE 1.

**FIGURE 2.**

Redox Potentials for Soluble Thiols in Visceral Yolk Sac, Yolk Sac Fluid, Amniotic Fluid and Embryo Following Exposure to Leupeptin for 26 hr in Whole Embryo Culture

*significantly different than control value, p , 0.05



*Soluble Relative Fluorescence
*Insoluble Relative Fluorescence

Values represent clearance of FITC from culture medium (μ l cleared /min/mg protein) in 3 hr.

FIGURE 3.
FITC-AI bum in Assessment of Histirotrophic Nutrition Activity
*significantly different than control value, p, 0.05

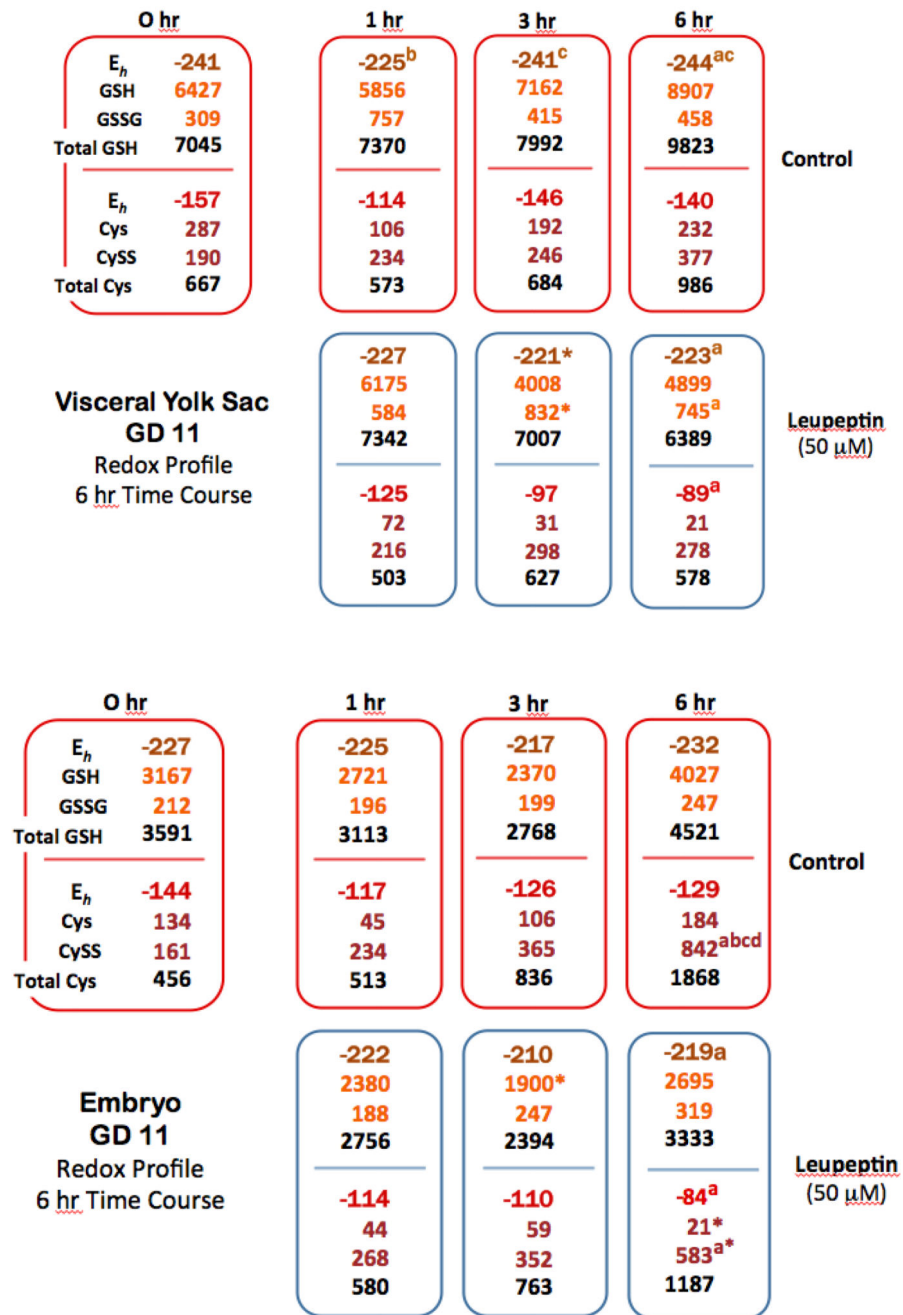
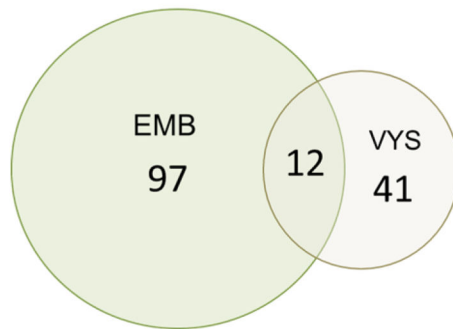
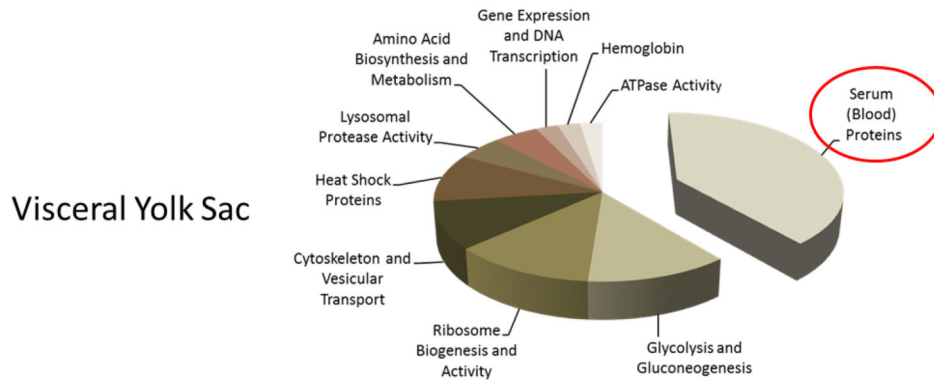


FIGURE 4.



Affected Proteins Common to Embryo and VYS	VYS	EMB
60 kDa heat shock protein, mitochondrial	1.17	0.65
Heat shock cognate 71 kDa protein	0.63	0.73
Heat shock protein HSP 90-alpha	0.77	0.65
Heat shock protein HSP 90-beta	0.72	0.68
Tubulin alpha-4A chain	1.34	0.60
Actin, cytoplasmic 1	1.26	0.84
Elongation factor 2	0.80	0.59
Pyruvate kinase isozymes M1/M2	0.57	1.20
Fructose-bisphosphate aldolase A	1.34	0.65
D-3-phosphoglycerate dehydrogenase	1.26	1.15
40S ribosomal protein S11	1.29	0.62
Nucleosome assembly protein 1-like 1	0.82	0.63

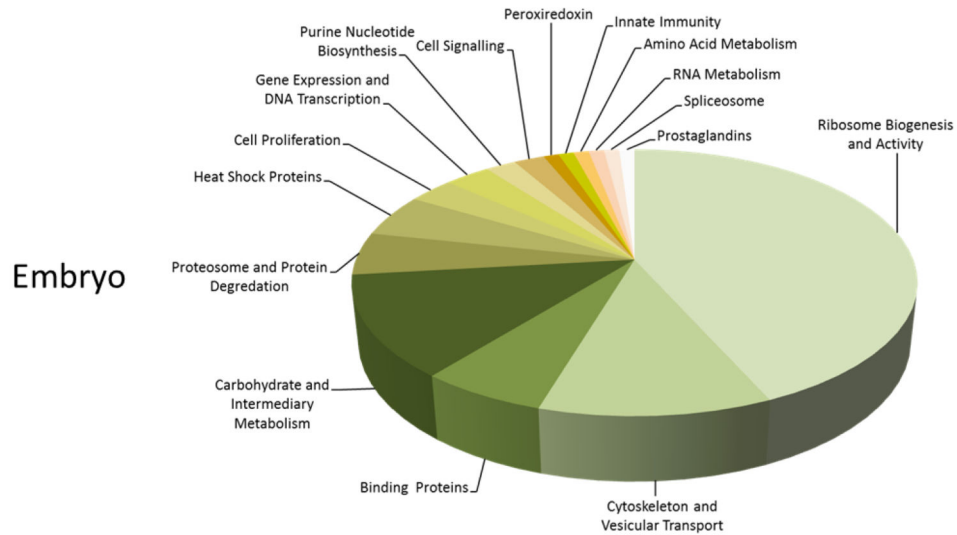


FIGURE 5.

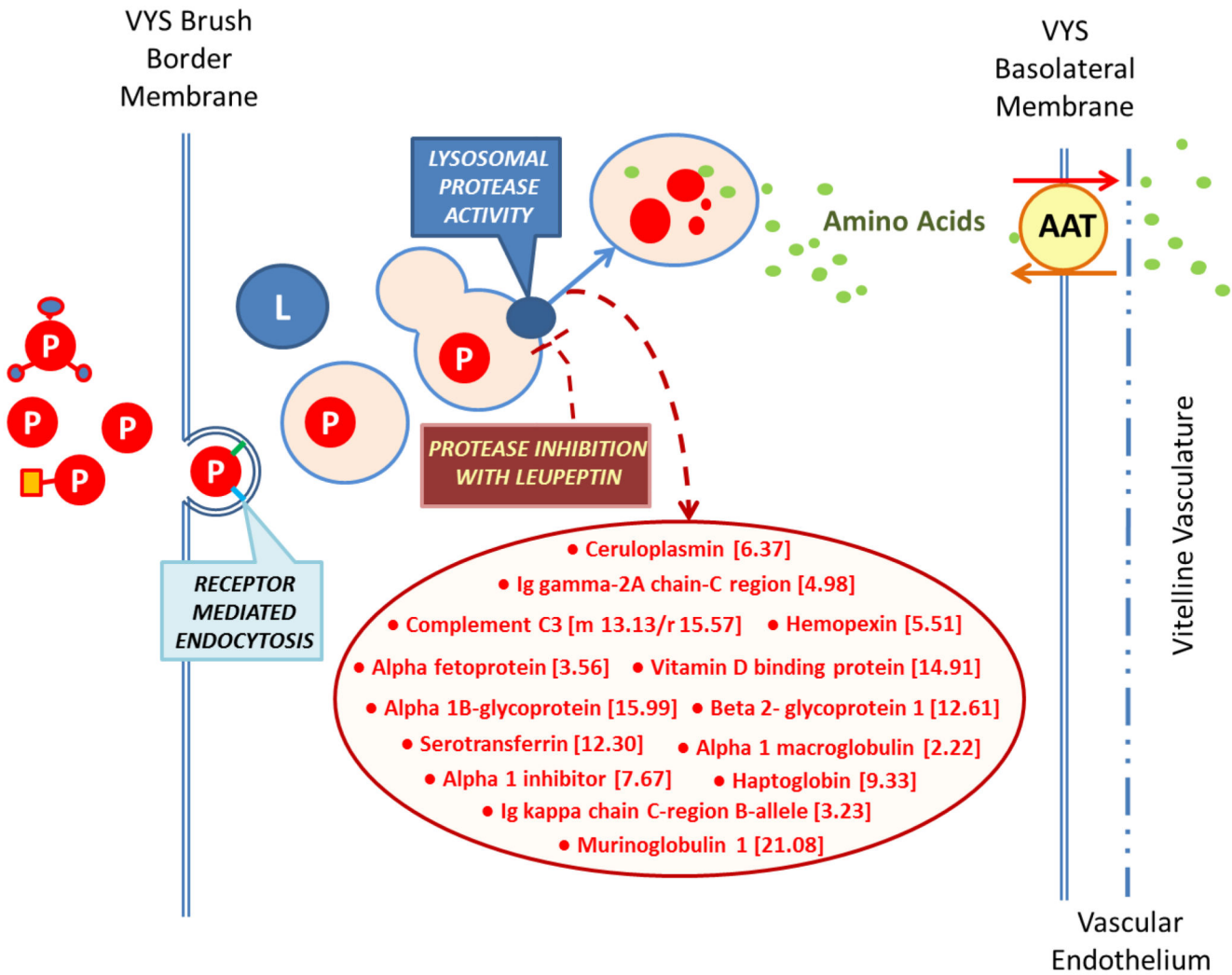


FIGURE 6.